Lecture notes
Boulder summer school 2015
Soft matter in and out of equilibrium

Geometric frustration and handedness

Efi Efrati

July 10, 2015

This series of three lecture will deal with two basic notions that are encountered in many different soft matter systems; geometric frustration and handedness. The first two lectures will focus on geometric frustration. We will introduce different kinds of geometric frustration, and discuss different possible strategies of resolving the resulting frustration, emphasizing differences between local and global strategies. The third lecture will introduce a quantitative path to handed phenomena. We will discuss the history of chirality as defined by Lord Kelvin, and the difficulties that arise when using it as a source for a quantitative treatment of handedness. We will then present the orientation dependent generalization of this notion, and its implications. Both notions, that of geometric frustration and that of handedness, are of exceptional use in may soft matter systems where the constituents of a structure are ofter big enough to possess a non-trivial internal structure.

1 Geometric frustration: Examples and Riemannian formulation

When a multicellular tissue grows or a ductile material irreversibly deforms, the different cells and different regions in the material may experience different conditions and thus deform differently. However, the restriction that the tissue remains connected and continuous, forces the different cells or parts of the material to fit next to one another. As the deformation profile was not necessarily programed to make the different parts snugly fit next to one another, this will result in frustration; the inability to simultaneously satisfy all intrinsic tendencies in the material (in the present case, matching all the rest-lengths).

This frustration is not always unwanted. It can be exploited to produce elaborate shapes from very simple inputs, as well as to strengthen the material against failure (for example in tempered gorilla glass covering our smart phones).

The resolution of geometric frustration may be local (resolving the frustration uniformly), or resolve the frustration globally, incorporating into the solution quantities of the object as a whole, such as total volume and aspect ratio.

In what follows we shall explore natural and man-made examples of geometric frustration, and understand how to treat such phenomena quantitatively. This will naturally require some use of differential geometry. I will introduce the notions needed for our discussion, but will do so not in the most general framework. The less restricted form of these derivations can be found in elementary differential geometry books (e.g. *Lectures on classical differential geometry* by Struik, and *Differential geometry* by Pogorelov. A more mathematically advanced account may be found in *An introduction to differential geometry with applications to elasticity* by Ciarlet). I also want to draw the participants' attention to the 2002 summer school lecture notes by Randy Kamien *"The geometry of soft materials: A primer"* which also saw light as a review article in Rev. Mod. Phys.

1.1 Examples of geometrically frustrated systems

1.1.1 Flattening the sphere

One of the most familiar notion of geometric incompatibility is that of flattening the sphere. For hundreds of years cartographers have been faced with the challenge of accurately describing the spherical surface of the earth on flat pieces of paper. We know that any such "flattening" will necessarily distort distances and shapes. There are two types of questions concerning such maps, the first is to find the most accurate way of mapping a region in space, and the second concerns the most accurate description of the whole globe. We will discuss both of these notions (termed local and global notions) of incompatibility, and will address the question of minimal distortion quantitatively.

1.1.2 Doubly curved bilayer: The Bauhinia seed-pod geometry

Next let us consider the following geometry: Two thin elastic sheets of thickness t are uniaxially stretched by a factor $1+\alpha$ with respect to each other along perpendicular directions and are then glued to one another. Along each direction we can estimate the difference in length between the center of the layers when curved to a radius R:

$$\frac{l_{out}}{l_{in}} = \frac{R+t/2}{R-t/2} = \frac{1+\alpha/2}{1-\alpha/2} \Rightarrow \kappa = R^{-1} = \frac{\alpha}{t}.$$

The curvature along the two directions is equal in magnitude but points along opposite directions (and thus associated with opposite signs). We note that we can keep R constant and take α to be arbitrarily small provided also diminish the thickness t accordingly. In this limit, we do not change the two dimensional geometry of each of the layers (which both start planar, and thus with

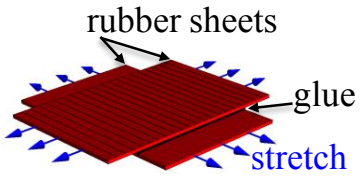

Figure 1: Constructing the doubly curved bilayer through gluing two oppositely tensed thin rubber sheets.

zero Gaussian curvature, $K = 0$). However, the desired geometry is associated with a non-vanishing Gaussian curvature $K = \kappa_1\kappa_2 = -R^{-2}$. Gauss' theorema egregium which relates the metric properties of a surface to its allowed conformation in space through the Gaussian curvature thus precludes the ability to simultaneously conform to the 2D geometry and the prescribed curvatures.

1.1.3 Bend-Splay coupling in 2D nematic liquid crystals

A two dimensional nematic liquid crystal is characterized by a unit vector field $\hat{\mathbf{n}}$ named the director which is indicative of a local preferred orientation of the constituents in the liquid. The constituents in a nematic liquid crystal, named *nematogens*, have a broken symmetry and are typically elongated rod-like structures. In its ground state a nematic liquid crystal attempts to align the nematogens, leading to a uniform and constant director field. However, this configuration may be distorted by imperfections, boundary conditions, and other external forces. The energetic cost of such deformations is given by the Frank free energy:

$$F = \tfrac{1}{2}K_s(\nabla \cdot \hat{\mathbf{n}})^2 + \tfrac{1}{2}K_b\left((\hat{\mathbf{n}} \cdot \nabla)\hat{\mathbf{n}}\right)^2.$$

The first term is called the splay term, and the second is called the bending term. We could define $s = |\nabla \cdot \hat{\mathbf{n}}|$ and $b = |(\hat{\mathbf{n}} \cdot \nabla)\hat{\mathbf{n}}|$ to obtain the energy in compact form:

$$F = \tfrac{1}{2}K_s s^2 + \tfrac{1}{2}K_b b^2.$$

A third term (called the saddle splay) can be written as the divergence of a function, and for simplicity was omitted above. In three dimensions the above terms naturally extend to their three dimensional forms and an additional term, named twist (or helicity) appears, $\frac{1}{2}K_T(\hat{\mathbf{n}} \cdot \nabla \times \hat{\mathbf{n}})^2$.

For an unconstrained liquid crystal it is easy to see that the Frank energy in 2D yields a trivial minimizer where $s = 0$ and $b = 0$. However if we now consider a nematogen of a slightly more structured form, say having a slight longitudinal bend, things may look different. Such a liquid crystal will possess a non-vanishing preferred spontaneous bend. Its Frank energy, given by

$$F = \tfrac{1}{2}K_s s^2 + \tfrac{1}{2}K_b(b - b_0)^2,$$

favors a zero splay configuration with a constant bend of value b_0, and one may naïvely expect that we should only consider small perturbations about this ground state. However, as we next show, there exists no ground state with vanishing splay and a constant bending.

Setting $\hat{\mathbf{n}} = (\cos(\theta), \sin(\theta))$, the vanishing splay requirement amounts to $\theta_y = \tan(\theta)\theta_x$. This gives for the bending the expression

$$b = \theta_x / \cos(\theta) = \theta_y / \sin(\theta).$$

This can be immediately shown to be incompatible with the no splay condition as

$$\theta_{xy} = -b \sin(\theta)\theta_y = -b^2 \sin^2(\theta) \neq b^2 \cos^2(\theta) = b \cos(\theta)\theta_x = \theta_{yx}.$$

The uniformly bent ground state is therefore frustrated and the ground state will inevitably contain some splay or display non-uniform bending.

1.1.4 2D axially symmetric exponential growth

Last let us consider a circular ring of N cells that produces a new layer of ΛN cells, where $\Lambda > 1$ every generation. Had Λ been equal to unity this would have resulted in a cylindrical tube. The restriction that $\Lambda > 1$ requires the perimeter of the next generation to be longer. This growth of the perimeter occurs at an increasing rate. The most a circular perimeter can grow between layer of height Δh is $\rho(s+\Delta h) - \rho(s) = 2\pi\Delta h$, which occurs when the growth is planar. Beyond this point no axially symmetric solution can continue to increase the perimeter at an accelerating rate. This is known as the finite horizon of the pseudosphere. Beyond this point, growth must lead to a strong symmetry breaking of the configuration.

1.2 Formulation of the problem via Riemanian geometry

We now come to make these notions of frustration quantitative within the framework of Riemannian geometry. The main tool in Riemannian geometry is the Riemannian metric, g. This is the tool with which infinitesimal distances are defined. The metric is given with respect to a set of coordinates x^α:

$$ds^2 = g_{ij} dx^i dx^j,$$

where above, and hereon-after we assume the Einstein summation convention where repeated indices in a product are summed over. On a smooth Riemannian manifold every point locally looks like Euclidean space. A general Riemannian space differs from Euclidean space in that the former does not require to support the parallel postulate which holds in Euclidean space (that to every straight line and every point not on the line there exists a single straight line that passes through the point and never intersects the line). This gives Riemannian manifolds all their exotic behavior. In particular it allows for something called non-holonomy or non-trivial parallel transport. For pedagogical reasons, in what follows next we will consider the notion of connection, covariant derivative, and parallel transport for surfaces embedded in 3D. Each of these notions can, of course, be defined in arbitrary dimensions and without the need to resort to an embedding.

Let us consider a surface in Euclidean three dimensional space,

$$\mathbf{r}(\mathbf{x}) = \big(r^1(x^1, x^2), r^2(x^1, x^2), r^3(x^1, x^2)\big).$$

The metric is obtained by examining infinitesimal displacements along the surface (dx^1, dx^2):

$$ds^2 = d\mathbf{r} \cdot d\mathbf{r} = \frac{d\mathbf{r}}{dx^\alpha} \cdot \frac{d\mathbf{r}}{dx^\beta} dx^\alpha dx^\beta = g_{\alpha\beta} dx^\alpha dx^\beta.$$

The inverse metric is also a useful tool in geometry

$$g^{\alpha\beta} = (g_{\alpha\beta})^{-1}, \quad \text{i.e.} \quad g_{\alpha\beta} g^{\beta\gamma} = g^{\gamma\beta} g_{\beta\alpha} = \delta^\gamma_\alpha.$$

A vector on the surface in our specific embedded context should be thought of as the possible velocity vector of a particle moving on the surface. It is a vector in $\mathbb{R}^3$ that is locally tangent to the surface. Such a vector can be defined through its contravariant (marked by upper indices) components, or through its covariant (marked by lower indices) components:

$$\mathbf{v} = v^\alpha \partial_\alpha \mathbf{r} = v_\beta g^{\alpha\beta} \partial_\alpha \mathbf{r} = v_\beta \partial^\beta \mathbf{r}$$

where $\partial_\alpha \mathbf{r} = \partial \mathbf{r} / \partial x^\alpha$ and $\partial^\alpha \mathbf{r} = g^{\alpha\beta} \partial_\beta \mathbf{r}$. We now are able to differentiate the components of a vector. We recall that the component of the vector at different points are defined with respect to different basis vectors. It thus will surprise us that a correction term should be introduced to compensate for this effect.

$$\partial_\alpha \mathbf{v} = \partial_\alpha v^\beta \partial_\beta \mathbf{r} + v^\beta \partial_\alpha \partial_\beta \mathbf{r} = (\partial_\alpha v^\beta + \Gamma^\beta_{\alpha\gamma} v^\gamma) \partial_\beta \mathbf{r} = (\nabla_\alpha v^\beta) \partial_\beta \mathbf{r},$$

where we have defined the Christoffel symbol: $\partial_\alpha \partial_\beta \mathbf{r} = \Gamma^\gamma_{\alpha\beta} \partial_\gamma \mathbf{r}$. This compensated differentiation is called the covariant derivative. Similarly one can show that for the covariant components the covariant derivative reads

$$\nabla_\alpha v_\beta = \partial_\alpha v_\beta - \Gamma^\gamma_{\alpha\beta} v_\gamma. \tag{1}$$

One can also easily show that the Chrisftoffel symbol can be calculated directly from the metric:

$$\Gamma^\gamma_{\alpha\beta} = \tfrac{1}{2} g^{\gamma\delta} (\partial_\alpha g_{\beta\delta} + \partial_\beta g_{\alpha\delta} - \partial_\delta g_{\alpha\beta}). \tag{2}$$

The Christoffel symbol is the central tool in defining the **connection** on the manifold, that is in determining how to compare vector in different locations, or alternatively in determining how to parallel translate vectors. The notion of parallel translation of a vector along a path is trivial in Euclidean space, "one only needs to keep the direction of the vector constant". This is because the connection in this case is trivial and directions can be defined globally. This is the case of general Riemannian geometry in which directions are cannot be defined globally. One can formulate the notion of parallel transport locally: Two parallel vectors in Euclidean space form with a given straight line a constant angle. Similarly, to infinitesimally translate a vector v_α along a path γ we simply construct at every point a geodesic curve that is locally tangent to the curve γ, and keep a constant angle between the vector and the geodesic. Unlike the case in Euclidean space, parallel translating a vector around a closed loop in a general Riemannian manifold results in a rotation which is proportional to the area enclosed by the loop. The local manifestation of this non-holonomy is the non-commutativity of second derivatives

$$\nabla_\alpha \nabla_\beta v_\gamma - \nabla_\beta \nabla_\alpha v_\gamma = R^\delta_{\gamma\alpha\beta} v_\delta,$$

where the Riemannian curvature tensor appearing above reads

$$R^\delta_{\gamma\alpha\beta} = \partial_\alpha \Gamma^\delta_{\beta\gamma} - \partial_\beta \Gamma^\delta_{\alpha\gamma} + \Gamma^\nu_{\beta\gamma}\Gamma^\delta_{\alpha\nu} - \Gamma^\nu_{\gamma\alpha}\Gamma^\delta_{\beta\nu}. \tag{3}$$

We now note that the central formulas above (3), (2) and (1) rely only on knowledge of the metric and do not require the specific embedding we used to understand the intuition behind these notion. Given a Riemannian metric we can paralle transport vector, define curvature, and use covariant differentiation as we wish.

In order to discuss physical properties of a manifold we will need to parameterize it. Naturally, many of the calculated quantities will depend on the specific parametrization. In particular, the components of the metric tensor and and of the christtoffel symbols will differ between different parametrizations. However, we will see that all relevant scalar quantities will be parametrization independent. If we contract a contravariant vector field v^α with a covariant vector field u_α the resulting scalar field $v^\alpha u_\alpha = \phi$ will be independent of the parametrization used (despite the fact that the component of both vector fields will depend on the parametrization). This will also bring us to conclude that when formulated properly, if a vectorial equation holds with respect to one parametrization, it will hold true for every parametrization despite the fact that the components of the vectors will strongly depend on the parametrization. Higher indexed quantities, such as the metric, are called tensors and should be thought of as an external product of vectors. We note in passing that the Christoffel symbol is not a tensor in this sense (and thus is not allowed into covariant equations), however the difference of two Christoffel symbols with respect to two different metrics is a tensor.

1.3 Existence and uniqueness of an embedding for flat metrics

Let us now consider a three dimensional flat manifold, again given by the mapping $\mathbf{r}(\mathbf{x})$. One could think of this structure as endowing space with curvilinear coordinates. Recalling that the Christoffel symbol reads

$$\partial_i \partial_j \mathbf{r} = \Gamma^k_{ij} \partial_k \mathbf{r}, \tag{4}$$

As we know that parallel transport is trivial in Euclidean space, we expect the Riemann curvature tensor to vanish. We can ask if that is a sufficient condition on the metric to produce such a flat manifold. The way to answer such a question is constructive. We try to reconstruct the manifold from knowledge of the metric alone. One could think of the definition of the Christoffel symbol above as a first order PDE for $\mathbf{V}_\alpha = \partial_\alpha \mathbf{r}$. Such a set of PDE's allows a solution only if $\partial_\alpha \partial_\beta \mathbf{V} = \partial_\beta \partial_\alpha \mathbf{V}$. Thus given a metric g_{ij}, and corresponding Christoffel symbols Γ^i_{jk} we can reconstruct from these a three dimensional structure in Eculidean space provided that

$$0 = \partial_j \partial_k \partial_i \mathbf{r} - \partial_k \partial_j \partial_i \mathbf{r} = (\partial_j \Gamma^m_{ik} - \partial_k \Gamma^m_{ij} + \Gamma^l_{ik} \Gamma^m_{lj} - \Gamma^l_{ij} \Gamma^m_{lk}) \partial_m \mathbf{r} = R^m_{ijk} \partial_m \mathbf{r}.$$

Which again implies vanishing of all coordinates of the Riemann curvature tensor. Thus a Riemannianly flat (vanishing curvature) 3D manifold can be has a unique realization in 3D Euclidean space (up to rigid motions).

1.4 Generation of incompatibility in non-uniform isotropic expansion

We now come to exemplify how difficult it is to construct a flat metric through a specific example. Consider a strain-free body, parameterized by Cartesian coordinates, i.e. $g = I$. Allow every point in the body to expand isotropically but non-homogeneously by a factor $\lambda(x)$, thus giving rise to a reference metric $\bar{g} = \lambda^2 I$. Such expansion may result for example from thermal expansion, or in growth induced by turgor pressure in plants' cells. We now ask a simple question: what isotropic growth profiles will result in a compatible reference metric, i.e. will be realizable by an Euclidean metric, g, and will therefore not induce residual stress?

To answer this question we write down the components of the Riemannian curvature tensor of the metric $\bar{g}$ in terms of the expansion factor λ and its derivatives. Taking independent linear combination of the covariant components of the Riemannian curvature tensor (essentially the components of the Ricci tensor $Ricci_{ij} = R^k_{ikj}$) yields the following compatibility conditions:

$$\begin{aligned}
&2(\partial_1\lambda)^2 - \lambda\partial_1\partial_1\lambda - \lambda\triangle\lambda = 0, \qquad && 2\partial_1\lambda\partial_2\lambda - \lambda\partial_1\partial_2\lambda = 0,\\
&2(\partial_2\lambda)^2 - \lambda\partial_2\partial_2\lambda - \lambda\triangle\lambda = 0, \qquad && 2\partial_1\lambda\partial_3\lambda - \lambda\partial_1\partial_3\lambda = 0,\\
&2(\partial_3\lambda)^2 - \lambda\partial_3\partial_3\lambda - \lambda\triangle\lambda = 0, \qquad && 2\partial_2\lambda\partial_3\lambda - \lambda\partial_2\partial_3\lambda = 0,
\end{aligned}$$

where $\triangle = \nabla \cdot \nabla = \partial_1^2 + \partial_2^2 + \partial_3^2$ is the standard Laplacian operator. It takes straightforward algebra and integration to find that the only non-constant solution of the above equations is

$$\lambda = \frac{C^2}{|\mathbf{x} - \mathbf{x_0}|^2},$$

for some constants C and $\mathbf{x_0}$. Every other isotropic expansion profile of an initially Euclidean 3D body will give rise to a non-Euclidean metric and inevitably result in a residually stressed body. This result, may be surprising when considering growth profiles. However it is a consequence of a well-known geometric result whereby all conformal mappings in $\mathbb{R}^3$ are inversions of a sphere. It implies that any growth that does not result in residual stress requires delicate global control, or some mechanical feedback.

1.5 Differential geometry of surfaces in three dimension

When coming to describe surfaces we will need to resort to slightly more complicated structures; namely the first and second fundamental forms. For surfaces embedded in three dimensions we distinguish between intrinsic properties (essentially the metric and quantities that can be derived from it) and extrinsic properties that can be changed without altering the metric, such as the principal curvature in a specific location. The latter properties will be said to depend on the specific embedding.

Given a surface $\mathbf{r}(x^1, x^2)$ and a surface normal $\hat{\mathbf{N}}$ we construct the first and second fundamental forms via

$$a_{\alpha\beta} = \partial_\alpha \mathbf{r} \cdot \partial_\beta \mathbf{r}, \qquad b_{\alpha\beta} = \partial_\alpha \partial_\beta \mathbf{r} \cdot \hat{\mathbf{N}}.$$

The second fundamental form measures curvature per unit of coordinate length. This is related to true length through the metric. A third tensor called the shape operator $c^\alpha_\beta = g^{\alpha\gamma} b_{\gamma\beta}$ gives curvatures in real units, independent of the parametrization. Two scalar quantities can be calculated from it; Its determinant is the Gaussian curvature $K = det(c) = \kappa_1\kappa_2$, and its trace is the mean curvature, $H = \frac{1}{2}(\kappa_1 + \kappa_2)$. Gauss' theorema egregium identifies the Gaussian curvature with the Riemannian curvature which can be calculated from the metric alone. This theorem naturally restricts the allowable pairs of fundamental forms. For example, the Eulidean metric $g = I$ cannot support a uniformly curved configuration $b = \kappa I$, or as we discussed in the examples a saddle like negative Gaussian curvature.

In addition to Gauss' equation there are two more differential restrictions on the fundamental forms These can be written compactly as

$$\nabla_\alpha b_{\beta\gamma} = \nabla_\beta b_{\alpha\gamma}.$$

The compatibility conditions for surfaces are called the Gauss-Peterson-Mainardi-Codazzi (GPMC) equations. Similarly to the case of Riemannian curvature

satisfaction of these equations is a necessary and sufficient condition for the existence of a unique surface with a given first and second fundamental forms. An exceptionally elegant derivation of these equations starts with a surface and extends it along its normal vector:

$$\mathbf{r}(x^1, x^2, x^3) = \boldsymbol{\rho}(x^1, x^2) + x^3 \hat{\mathbf{N}}(x^1, x^2)$$

The resulting metric g^{3D} can be expressed in terms of the 2D metric and curvature tensors, a and b:

$$g^{3D} = \begin{pmatrix} a - 2x^3 b & & 0 \\ & & 0 \\ 0 \quad 0 & & 1 \end{pmatrix} + \mathcal{O}((x^3)^2)$$

Calculating the Riemannian curvature tensor of g^{3D} reproduces the GPMC equations.

1.6 Homework assignment (optional)

Derive the compatibility condition for splay-free bending in a 2D liquid crystal.

1.7 Homework assignment solution: Splay-free bending in 2D liquid crystals

We start by setting as before $\hat{\mathbf{n}} = (\cos(\theta), \sin(\theta))$, and express the splay and bend terms explicitly:

$$\begin{aligned} s =& \nabla \cdot \hat{\mathbf{n}} = \partial_x n_x + \partial_y n_y = -\sin(\theta)\theta_x + \cos(\theta)\theta_y \\ b =& |(\hat{\mathbf{n}} \cdot \nabla)\hat{\mathbf{n}}| = \left(\sin(\theta)^2(\cos(\theta)\theta_x + \sin(\theta)\theta_y)^2 + \cos(\theta)^2(\cos(\theta)\theta_x + \sin(\theta)\theta_y)^2\right)^{\frac{1}{2}} \\ &= \cos(\theta)\theta_x + \sin(\theta)\theta_y \end{aligned} \tag{5}$$

These relations may of course be inverted to yield

$$\theta_y = \cos(\theta)s + \sin(\theta)b\,, \quad \theta_x = -\sin(\theta)s + \cos(\theta)b\,. \tag{6}$$

Requiring equality of the second mixed derivatives, $\theta_{xy} = \theta_{yx}$, gives

$$\begin{aligned} 0 =& s^2 + b^2 + n_y s_y + n_x s_x - n_x b_y + n_y b_x \\ =& s^2 + b^2 + \hat{\mathbf{n}} \cdot \nabla s - \hat{\mathbf{n}} \times \nabla b = 0. \end{aligned} \tag{7}$$

The fulfillment of this equation is necessary for the existence of a director field with a given bend and splay functions. For example we can show that the restriction to spatially uniform solutions (in which all derivatives vanish identically) results in

$$0 = s^2 + b^2,$$

allowing only the trivial solution.

It is important to state that equation (7) is not a compatibility equation in the classical sense as it contains the function θ (whose existence is sought) explicitly. Only completely eliminating it from the above equation will result in an autonomous condition. We next do this for the splay-free case.

Setting $s = 0$ and $\eta = 1/b$ equation (7) reduces to

$$1 = \sin(\theta)\eta_x - \cos(\theta)\eta_y. \tag{8}$$

Equation (8) yields

$$\sin(\theta) = \frac{\eta_x \pm \eta_y\sqrt{\eta_x^2 + \eta_y^2 - 1}}{\eta_x^2 + \eta_y^2}, \qquad \cos(\theta) = \frac{-\eta_y \pm \eta_x\sqrt{\eta_x^2 + \eta_y^2 - 1}}{\eta_x^2 + \eta_y^2}. \tag{9}$$

These equations in turn may be substituted into the definitions of the splay and bend

$$0 = s = \partial_x \cos(\theta) + \partial_y \sin(\theta), \qquad 1/\eta = \partial_x \sin(\theta) - \partial_y \cos(\theta).$$

The resulting two second order PDE contain only the variable η and their satisfaction is necessary for the existence of a director field $\hat{\mathbf{n}}$ with vanishing splay and bending given by $b = 1/\eta$. The converse is also established, i.e. the satisfaction of these equations is also sufficient in order to show the existence of such a director field.

2 Elasticity of frustrated structures

The purpose of this lecture is to complement the discussion of elasticity of the previous lectures and extend it to residually stressed solids. While the physical quantities we will deal with will be identical to those discussed in previous lectures, in the context of residually stressed solids it is of great use to formulate these in purely geometric means.

2.1 examples of frustrated elastic systems

We would like to start by reviewing several instances of residually stressed systems. The first structure is that of tempered glass. Almost all modern smart phones are covered with "Gorilla glass" an exceptionally thin tempered glass sheet. This greatly strengthens the glass against scratching and breakage. The side windows in our car are also tempered. In the case of car windows one not only wants to strengthen the glass against breakage but also to make sure that when the glass does break it leaves behind no large shreds.

In order to understand how tempering serves both these purposes we need to understand what is the mechanical state of tempered glass. The process of glass tempering usually follows in two steps. In the first step the glass in its final form is heated to allow flow. It is then cooled abruptly using forced air drafts. This solidifies the outer surfaces of the glass while the bulk of the glass remains molten and hot. During the gradual cooling the bulk shrinks. However, as the external surfaces have already solidified the bulk is held tensed. This tension is balanced by a corresponding compression on boundary. As brittle failure advances cracks under tension, compressing the exposed boundary of a body implies that in order to propagate a crack through the material one needs to first overcome the surface compression. However, this compression is balanced by very strong tension in the interior of the material. If for some reason this tensed region would be exposed, and thus allow a crack to nucleate the tensed interior would propagate the crack without any external forces. This often results in many cracks.

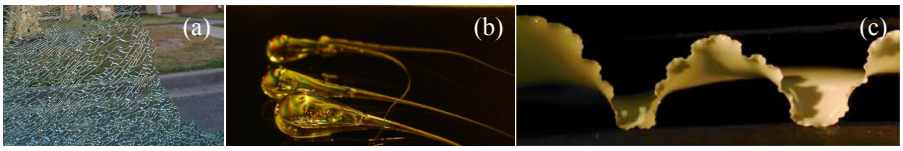

Figure 2: (a) A broken tempered glass. (b) Prince Rupert's drops, an extreme example of tempered glass. (c) A torn plastic sheet.

Torn thin plastic sheets provide another example of frustrated elastic structures. The tearing process is completely symmetric across the thin sheet. This "up/down" symmetry leads to inducing no curvatures. However, the resulting

torn edge is very bent and ruffled. This is due to the differential elongation near the crack tip. Regions closest to the torn edge have elongated the most along the tear direction, while region far away from the tear experience no irreversible deformation. This differential stretching induces a hyperbolic metric on the sheet. It is the embedding of this sheet that necessitates the ruffling of the edge. Such sheets, which are associated with a non-Euclidean metric yet have no intrinsic bending tendencies (much like thin plates) are called non-Euclidean plates, and will be treated in what follows.

2.2 Elasticity of amorphous frustrated structures

Having observed how easily (and almost inevitably) geometric frustration arises in continuous systems we may ask how can one treat such bodies elastically. For example, how can we describe elastic deformations in a differentially growing tissue. The abstract framework for such a description is that of hyperelasticity. In this framework the stress is assumed to be derived from an elastic energy function that depends only on the local deformation. Such ideally elastic material can show no history dependence are non-dissipative, and their constitutive relation (between stress and strain) is local. The main hurdle to overcome when applying this description to frustrated systems is the inability to define a stress-free configuration with respect to which strains will be measured. The classical theory of elasticity starts by defining the displacement vector mapping a stress-free configuration $\mathbf{x}$ to a deformed configuration $\mathbf{r}$, namely $\mathbf{u} = \mathbf{r} - \mathbf{x}$, and uses this displacement vector to define the strain tensor via

$$\epsilon_{ij} = \tfrac{1}{2}\left(\partial_i u_j + \partial_j u_i + \partial_i u_k \partial_j u_k\right),$$

where $\partial_i = \partial/\partial x^i$. However, when no stress-free configuration exists such a measure of the deformation is not available to us. We note however that

$$\begin{aligned}
\epsilon_{ij} =& \tfrac{1}{2}\left(\partial_i(r_j - x_j) + \partial_j(r_i - x_i) + \partial_i(r_k - x_k)\partial_j(r_k - x_k)\right), \\
=& \tfrac{1}{2}\left(\partial_i r_j - \delta_i^j + \partial_j r_i - \delta_i^j + (\partial_i r_k - \delta_k^i)(\partial_j r_k - \delta_k^j)\right) \\
=& \tfrac{1}{2}\left(\partial_i r_j - \delta_i^j + \partial_j r_i - \delta_i^j + (\partial_i r_k - \delta_k^i)(\partial_j r_k - \delta_k^j)\right) \\
=& \tfrac{1}{2}\left(\partial_i r_k \partial_j r_k - \delta_i^j\right) = \tfrac{1}{2}\left(g_{ij} - I_{ij}\right).
\end{aligned}$$

Thus the strain may be interpreted as a difference between the metric in the deformed state and the Euclidean metric of the stress-free reference state. If one maps the above definition of the strain to an alternative coordinate system $\mathbf{x}'$ such that $\partial x^i/\partial x'^j = \Lambda^i_j$ we obtain

$$\epsilon'_{ij} = \tfrac{1}{2}\left(g'_{ij} - \bar{g}_{ij}\right),$$

where $g'_{ij} = \Lambda^k_i g_{kl} \Lambda^l_j$ and $\bar{g}_{ij} = \Lambda^k_i \Lambda^k_j$. Note that the Riemann curvature of both metric tensors g and $\bar{g}$ are expected to vanish as they both describe metrics of bodies in Euclidean space. This new way of writing the strain, while slightly

more cumbersome to write, allows an immediate generalization of the elastic description to frustrated objects. The strain is simply the difference between the realized metric of the body g and some reference metric $\bar{g}$. As g describes a realization of a body in Euclidean space its Riemannian curvature tensor has to vanish. We recall that such a metric defines a configuration of the body uniquely (up to rigid motions), and thus can be used to fully describe the state of the examined body. We do not, however, pose any restrictions on $\bar{g}$. In particular whenever the Riemann curvature of the metric $\bar{g}$ is non-vanishing the object it describes has no stress free configuration.

The above leads to a generalization of the principle of hyper-elasticity:
The elastic energy stored within a deformed elastic body can be written as a volume integral of a local elastic energy density that depends only on (i) the local value of the metric tensor and (ii) local metrial properties that are independent of the configuration.

Under the assumptions that both space and the elastic body are homogeneous and isotropic and that strains are small we obtain

$$E = \int_\Omega \mathcal{W}(g, \bar{g}) \sqrt{|\bar{g}|} dx^1 dx^2 dx^3,$$

where the energy density is given by

$$\mathcal{W} = A^{ijkl} \epsilon_{ij} \epsilon_{kl} + \mathcal{O}(\epsilon^3),$$

and the elasticity tensor may be expressed entirely in terms of the reference metric and the two elastic response coefficients: the Young's modulus, Y and the Poisson ratio ν:

$$A^{ijkl} = \tfrac{Y}{1+\nu} \left(\frac{1}{2} \left(\bar{g}^{ik} \bar{g}^{jl} + \bar{g}^{il} \bar{g}^{jk} \right) + \tfrac{\nu}{1-2\nu} \bar{g}^{ij} \bar{g}^{kl} \right).$$

The stress may be obtained from the elastic energy density

$$S^{ij} = \frac{\partial \mathcal{W}}{\partial \epsilon_{ij}} = A^{ijkl} \epsilon_{kl} = \tfrac{Y}{1+\nu} \left(\epsilon^{ij} + \tfrac{\nu}{1-2\nu} \bar{g}^{ij} \epsilon^k_k \right).$$

This description recovers the familiar elastic description of regular bodies when substituting $\bar{g} = I$. However, its main advantages is in cases where $\bar{g}$ is non-Euclidean, where it gives rise to residual stress.

In the absence of external forces the field of residual stress must be self balancing. This property poses restrictions on the possible states of residual stress within a body. The restrictions for the field of residual stress may be obtained by considering a scalar field χ with a non vanishing gradient $v_i = \nabla_i \chi$, which satisfies

$$\nabla_i v_j = \nabla_i \nabla_j \chi = 0, \tag{10}$$

where the covariant derivative above is taken with respect to the metric g. For all such test functions χ the quadratic form $S^{ij} v_i v_j$ must average to zero when integrated over the entire body, i.e.,

$$\int_\Omega v_i v_j S^{ij} \sqrt{|\bar{g}|} dx^1 dx^2 dx^3 = 0. \tag{11}$$

The proof follows immediately from integration by parts and explicit substitution of the divergence equation for the stress. In particular, as the integrand is a quadratic form in the gradient, v_i, every non trivial residual stress field must contain both tension and compression.

2.3 Incompatibility and residual stress: A uniformly frustrated system

In this section we demonstrate the main difference between residual stress and residual strain. While the latter is a local property, the former depends also on global properties such as the domain size and shape.

Let $\bar{g}$ be a reference metric corresponding to a uniform Gaussian curvature, $\bar{K}$. We now seek an elastic energy minimizing configuration in the space of constant Gaussian curvature, $K = const$. We assume the domain of consideration and the parametrization such that both the reference metric and the embedding metric g are uniformly close to the Euclidean metric, $|\bar{g} - I| \leq \delta$, and $|g - I| \leq \delta$.

To leading order in δ the divergence equation reduces to the cartesian divergence equation.

$$\partial_i S^{ij} = 0,$$

which implies the existence of a scalar function Φ (Airy stress potential) such that

$$\partial_1 \partial_1 \Phi = S_{22}, \quad \partial_2 \partial_2 \Phi = S_{11}, \quad \partial_1 \partial_2 \Phi = -S_{12}.$$

For simplicity we now consider a material with a vanishing Poisson ratio and set the Young's modulus to unity. In such a case the Bilaplacian of the scalar function reads

$$\triangle^2 \Phi = \bar{K} - K = -\Delta K,$$

where we have made use of the linearized Gaussian curvature (in leading order in δ) where by

$$K = -\tfrac{1}{2}(\partial_1 \partial_1 g_{22} + \partial_2 \partial_2 g_{11} - 2\partial_1 \partial_2 g_{12}).$$

Note the symmetry between embedding a hyperbolic surface in Euclidean space and the embedding of a flat surface on a positively curved space. We now consider a strip of length L and width w such that $w << L << L_{geo}$ where L_{geo} is the smallest geometric lengthcale associated with the curvatures; $\frac{1}{\sqrt{K}}$ and $\frac{1}{\sqrt{\bar{K}}}$. Assuming that away from the boundaries the solution will not depend on the coordinate along the long direction, x^2, we obtain

$$S_{11} = S_{12} = 0, \qquad S_{22} = -\frac{\Delta K}{2}\big((x^1)^2 - \frac{w^2}{12}\big).$$

The value of the constant above was set to by requiring the stress to have a vanishing average in the range $-w/2 \leq x^1 \leq w/2$. Upon integration we obtain for the elastic energy

$$E \propto w^5 L (\Delta K)^2.$$

The above scaling reads $E \propto w^4 A$ for strips of constant width and varying area, and scales as $E \propto \alpha^2 A^3$ for strips of constant aspect ratio $\alpha = w/L$. One can also solve the above equations is cylindrical geometry to recover the constant aspect ratio scaling $E \propto A^3$ under the assumption of axial symmetry.

2.4 Dimensionally reduced theory for frustrated thin sheets

We studying slender three dimensional bodies having one small dimension we would like to describe their state and response through surface properties. This is the motivation behind dimensionally reduced 2D elasticity models such as the Foppl Von Karman theory or the Koiter theory for thin plates. For frustrated this structures we can follow similar lines and obtain a dimensionally reduced functional for frustrated thin elastic structures.

For a given thin body we choose a parametrization such that $x^3 = 0$ defines the mid-surface in the body and the x^3 variable extend perpendicularly to the surface. This leads to a consideration of the body as composed of laminae (each characterized by its x^3 value). In this case the metric reads:

$$\bar{g} = \begin{pmatrix} \bar{g}_{11} & \bar{g}_{12} & 0 \\ \bar{g}_{21} & \bar{g}_{22} & 0 \\ 0 & 0 & 1 \end{pmatrix}.$$

Here $x^3 \in [-t/2, t/2]$, where t is the local thickness. We define the reduced two dimensional reference fundamental forms

$$\bar{a}_{\alpha\beta} = \bar{g}_{\alpha\beta}\big|_{x^3=0}, \qquad \bar{b}_{\alpha\beta} = -\tfrac{1}{2}\partial 3 \bar{a}_{\alpha\beta}\big|_{x^3=0}.$$

Using the reference fundamental forms we may express the three dimensional elastic energy in terms of a two dimensional energy density

$$\begin{aligned} E &= \int\int\int \mathcal{W}(g, \bar{g}) \sqrt{|\bar{g}|} dx^1 dx^2 dx^3 \\ &\approx \int\int \mathcal{W}^{2D}(a, \bar{a}, b, \bar{b}) \sqrt{|\bar{a}|} dx^1 dx^2. \end{aligned}$$

Carrying out a formal expansion of the elastic energy density in powers of the thickness, we obtain a reduced energy density,

$$\mathcal{W}^{2D}(x^1, x^2) = t e_S(x^1, x^2) + t^3 e_B(x^1, x^2), \tag{12}$$

where

$$\begin{aligned} e_S(x^1, x^2) &= \frac{1}{8} \mathcal{A}^{\alpha\beta\gamma\delta} (a_{\alpha\beta} - \bar{a}_{\alpha\beta})(a_{\gamma\delta} - \bar{a}_{\gamma\delta}) \\ e_B(x^1, x^2) &= \frac{1}{24} \mathcal{A}^{\alpha\beta\gamma\delta} (b_{\alpha\beta} - \bar{b}_{\alpha\beta})(b_{\gamma\delta} - \bar{b}_{\gamma\delta}), \end{aligned}$$

and the reduced two dimensional elastic tensor is

$$\mathcal{A}^{\alpha\beta\gamma\delta} = \tfrac{Y}{1+\nu} \left[\tfrac{1}{2} (\bar{g}^{\alpha\gamma} \bar{g}^{\beta\delta} + \bar{g}^{\alpha\delta} \bar{g}^{\beta\gamma}) + \tfrac{\nu}{1-\nu} \bar{g}^{\alpha\beta} \bar{g}^{\gamma\delta} \right].$$

The elastic problem is defined as follows: given two reference fundamental forms $\bar{a}$ and $\bar{b}$ find the realized fundamental form by minimizing the elastic energy among all first and second fundamental forms that satisfy the compatibility conditions:

$$\begin{aligned} \partial_2 b_{11} - \partial_1 b_{12} &= b_{11}\Gamma^1_{12} + b_{12}(\Gamma^2_{12} - \Gamma^1_{11}) - b_{22}\Gamma^2_{11} \\ \partial_2 b_{12} - \partial_1 b_{22} &= b_{11}\Gamma^1_{22} + b_{12}(\Gamma^2_{22} - \Gamma^1_{12}) - b_{22}\Gamma^2_{12} \\ b_{11}b_{22} - b^2_{12} &= K(a_{11}a_{22} - a^2_{12}), \end{aligned} \tag{13}$$

2.5 Non Euclidean plates

We now come to examine specific examples of frustrated thin elastic sheet. The first type will resemble flat plates in the sense that is is composed of identical laminae across its thickness, and thus favors flat configurations . This implies $b_{\alpha\beta} = 0$. When the 2D metric of such thin bodies is non-Euclidean (and thus necessitating curvatures), they are called non-Euclidean plates. The torn plastic sheets are an example of an uncontrolled production of such non-Euclidean plates. A more controlled version mad in hydrogel can be found in figure 3.

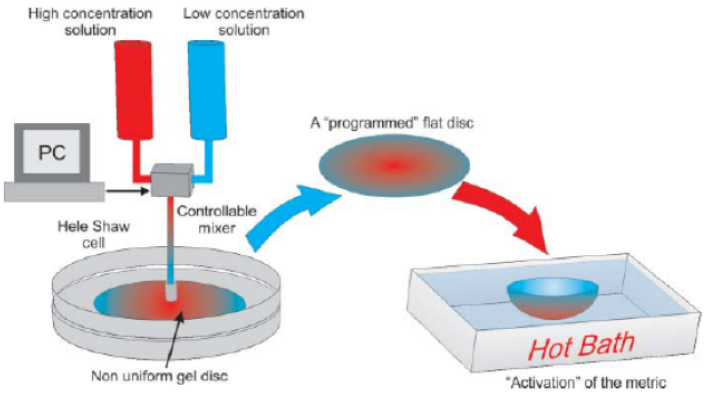

Figure 3: A hydrogel system for the controlled production of axially symmetric non-Euclidean plates. A mixture of high and low concentration thermally responsive gel is injected into a Hele-Shaw cell and is polimerized and cross linked freezing the concentration gradients in the material. When heated low concentrations regions shrink significantly more that high concentration region endowing the gel with a non-Euclidean 2D metric. As there is no structure along the thin dimension, the only shaping mechanism in this case is the metric. Image from Klein et-al, Science 2007.

We can use the hydrogel setting to create a non-Euclidean plate with the metric of a hemisphere. Below we describe its behavior as a function of thickness. This description remains valid form all kinds of non-Euclidean plates. For large

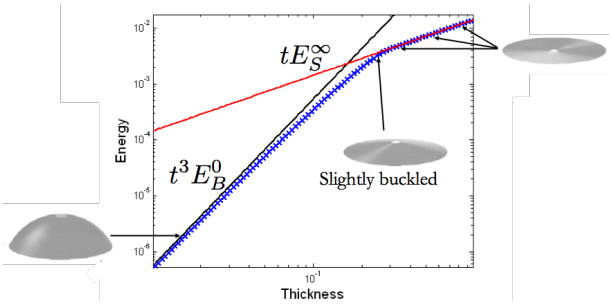

Figure 4: The elastic energy of a hemispherical non Euclidean plate as a function of the thickess.

thickness bending energy is expensive and a planar solution is favored. As the thickness is lowered bending becomes more favorable with respect to stretching and at a critical thickness the thin sheet buckles out of the plane. This reduces its stretching energy, but increases its curvature. As the thickness is further diminished the metric of the thin sheets approaches the reference metric and the surface accumulates more and more bending. In the vanishing thickness limit, bending is infinitely more energetically favorable than stretching and the obtained conformation is an isometric embedding of the reference metric.

One could easily show that for example the bending content is a monotonically decreasing function of the thickness (increasing with diminished thickness). We start by identifying the elastic energy minimizing configuration $r^*(t)$ for every thickness, t:

$$te_S(r^*(t)) + t^3 e_B(r^*(t)) = E(r^*(t), t) = E^*(t) = \min_r E(r, t).$$

We now note that the minimizer $r^*(t)$ has the least amount of energy compared to all other possible configurations at thickness t. This for example implies that $E(r^*(t), t) \leq E(r^*(t+\Delta), t)$ and that $E(r^*(t+\Delta), t+\Delta) \leq E(r^*(t), t+\Delta)$. Substituting we obtain

$$\begin{aligned} e_S(r^*(t)) + t^2 e_B(r^*(t)) \leq & e_S(r^*(t+\Delta)) + t^2 e_B(r^*(t+\Delta)), \\ e_S(r^*(t+\Delta)) + (t+\Delta)^2 e_B(r^*(t+\Delta)) \leq & e_S(r^*(t)) + (t+\Delta)^2 e_B(r^*(t)), \end{aligned}$$

which when subtracted gives

$$((t+\Delta)^2 - t^2) e_B(r^*(t+\Delta)) \leq ((t+\Delta)^2 - t^2) e_B(r^*(t)).$$

Thus for positive Δ we obtain $e_B^*(t+\Delta) \leq e_B^*(t)$.

We note again that for frustrated systems the zero energy level sets of the two energy terms e_S and e_B have no overlap. One particular outcome of this is the loss of equipartition. In general when an energy is composed of two quadratures we expect some notion of equipartition; that energy variation in the first term

is balanced (at equilibrium) by the energy variation of the second term. While the latter statement naturally hold in our system:

$$0 = \left.\frac{\delta E(\mathbf{r},t)}{\delta \mathbf{r}}\right|_{\mathbf{r}^*(t)} = t\left.\frac{\delta e_S(\mathbf{r})}{\delta \mathbf{r}}\right|_{\mathbf{r}^*(t)} + t^3\left.\frac{\delta e_B(\mathbf{r})}{\delta \mathbf{r}}\right|_{\mathbf{r}^*(t)} \Rightarrow t\dot{e}_S^* = -t^3\dot{e}_B^*,$$

where the last equality follows from multiplying by $\dot{\mathbf{r}}^*(t)$. However, when $e_S^* = 0$ (in the vanishing thickness limit) we have $e_B^* = e_B^0 > 0$. This implies that the two terms may obey different scaling laws (and thus not balance each other out).

If, for example, $e_S^*(t) \propto t^\alpha$ then $e_B - e_B^0 \propto -t^{\alpha-2}$. This means that for $\alpha > 2$ the dominant behavior for small thickness satisfies $te_S^* \propto t^{\alpha+1}$ whereas $t^3 e_B^* \propto e_B^0 t^3$. For surfaces embeddable with finite bending energy one can show that $\alpha = 5/2$ and is due to a boundary layer contribution, where in a region whose width scale as $\sqrt{t/\kappa_\parallel}$ the sheet behaves as if it is thick.

2.6 Shaping by curvature prescription

The complementary problem to the shaping by metric prescription of non-Euclidean plates is shaping by curvature prescription. In the former, $\bar{b}_{\alpha\beta} = 0$ is trivial but the metric is associated with a non-vanishing Gaussian curvature $\bar{K} \neq 0$. In the latter, which will be discussed here, the metric is trivial $\bar{a} = I$, but the reference curvatures will be non-trivial.

For the rubber bilayer described in Figure 1 we obtain

$$\bar{a} = \begin{pmatrix} 1 & 0 \\ 0 & 1 \end{pmatrix}, \quad \text{and} \quad \bar{b} = \begin{pmatrix} \kappa & 0 \\ 0 & -\kappa \end{pmatrix}.$$

In the thin limit our surface must be Riemannianly flat (and thus cannot curve in two dimensions simultaneously). It therefor assumes one of two cylindrical conformations in which one of the reference principal curvatures is obeyed, while the other is compromised. In the thick limit the curvature is obeyed and the metric is compromized.

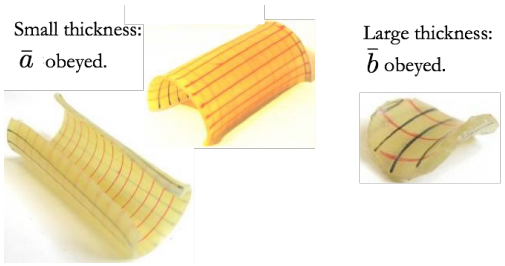

Figure 5: A thin elastic sheet shaped by curvature prescription prepared as described in Figure 1. Both the thin and thick limit are accessible. The transition between the two limits, unlike the non-Euclidean plates case, does not occur through a buckling transition but is continuous. Note the boundary layer visible at the free edge of the isometric configurations. Image adapted from Armon et-al, Science 2011.

3 Handedness quantification

The quantification of handedness is elusive. While it is a very intuitive notion, and one can easily classify a screw to be right handed or left handed, the general quantification of handedness has been a long standing challenge. We will try to elucidate these difficulties, and show how examining single particles in well defined orientations, a task made possible only by very recent technological advancements, has guided the path to a consistent quantification scheme.

3.1 A brief historical review

In 1811 the french scientist Francois Arago, only 25 years old at the time, is the first to discover the optical activity of quartz crystals. The term optical activity, synonymous with circular dichroism, describes the turning of the direction of polarization of linearly polarized light about its direction of propagation. This phenomenon may be understood as arising from a difference in the indices of refraction for right handed circularly polarized light and left handed circularly polarized light (as identified by Fresnel in 1824). It is thus a very close relative of linear birefringence where the different linear polarizations are associated with different indices of refraction. In most cases however, the linear birefringence component is going to be considerably larger than the circular birefringence. For this reason circular birefringence was first observed in settings where structural symmetry or isotropic arrangement of the constituents eliminate the linear birefringence component.

One puzzle that arose from the intensive study of the optical activity in organic solutions was the that of the optical properties of tartaric acid. Tartaric acid is one of the three main acids in red wine, and sometimes appears on the bottom of the cork in the form of small crystals. When tartaric acid is extracted from wine lees it is optically active, strongly rotating light counterclockwise when approaching an observer. However, when synthesized artificially in a lab the resulting tartaric acid is not optically active, despite having the exact same composition. This puzzle was resolved in 1847 by Louis Pasteur who discovered that, unlike the common thought at the time, the structure of tartaric acid crystals produced by wine lees is different from the structure of those produced in the lab. In particular when artificially synthesized tartaric acid is crystallized two types of crystals form. One of these structures is identical to the one obtained when crystalizing tartaric acid produced by wine lees. The other structure is its mirror image. The two differ by the location of one of the small facets, a difference overlooked until Pasteur's study. Pasteur separated the two types of crystals and redissolved them separately. The obtained solutions showed strong (and opposite) optical activity. Pastuer not only deduces that the optical activity and crystal geometry are a common manifestation of an underlying handed molecular structure but arrived at far reaching conclusions about the role of handedness in biology and life:
"I am inclined to think that life, as manifested to us, must be a function of the dissymmetry of the universe and of the consequences it produces...Life is

dominated by dissymmetrical actions. I can even foresee that all living species are primordially, in their structure, in their external forms, functions of cosmic dissymmetry. "

It is this context, of handedness manifesting in the optical activity of isotropic solutions and owing to a yet unrevealed underlying structure that we should interpret the definition of handedness. This definition was given by Lord Kelvin in his Baltimore lectures in 1893:
"I call any geometrical figure, or a group of points, chiral, and say that it has chirality if its image in a plane mirror, ideally realized, cannot be brought to coincide with itself."

3.2 Difficulties in quantitative chirality

There are several challenges one faces in coming to construct a quantitative measure of handedness following Lord Kelvin's definition of Chirality. First, object that one would like to assign handedness to, are found to be achiral. For example there are four crystal groups that are achiral (i.e. they are superposable on their mirror image) but can support optical activity. Moreover even very intuitively handed response properties such as the counterclockwise rotation of a four cup anemometer (a device for measuring wind velocity) cannot be attributed to an underlying handed structure of the anemometer as it possesses a plane of mirror symmetry.

A more abstract, but perhaps more devastating difficulty comes from the notion of chiral connectedness. In 1997 it was shown by Weinberg and Mislow that in D dimensions if a body has $D+2$ degrees of freedom or more one could continuously distort the conformation of the body into its own mirror image without ever passing through a mirror symmetric configuration. A quantitative measure following Lord Kelvin's definition of chirality is expected to read zero only if an object is mirror symmetric, and change sign under reflections. The notion of chiral connectedness precludes the existence of a such a continuous measure.

3.3 Handedness in mirro symmetric objects

The rubber sheet bi-layer discussed earlier this week provides a particularly useful example of a mirror symmetric structure giving rise to handedness. Its internal structure is homogeneous in the plane and symmetric under reflections. However, when long and narrow strips are cut from the bilayer they curve to form helicoidal strips of both right and left handedness depending on the relative orientation of the strips and the directions in which the layers were stretched. Strips whose long direction is oriented along the $x-$axis form right handed helicoids whereas strips whose long direction is oriented along the $y-$axis form left handed helicoids. The symmetric square cutout (c.II), as expected, gives rise to no distinct handedness. However, it is capable of manifesting extrinsic handedness when considered in specific directions, right along the $\pm x$ directions

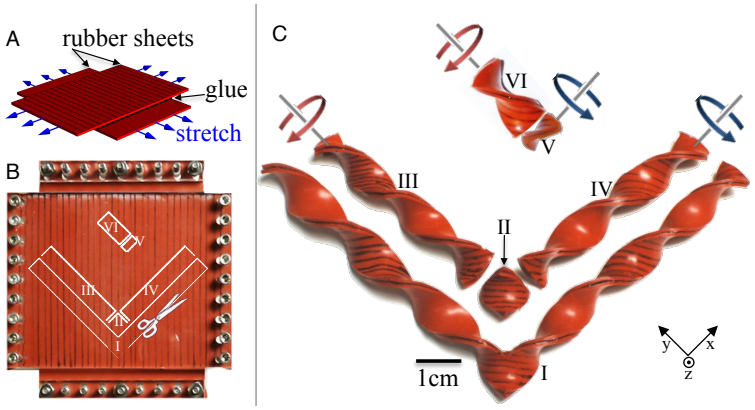

Figure 6: *Orientation dependent manifestation of handedness in a reflection symmetric continua.* Two identical rubber sheets are uniaxially stretched and glued together to form a rubber bilayer. Narrow strips cut from the bilayer curve out of plane to accommodate the difference in rest length between the layers and form helical structures. The square boundaries in b.II give rise to a cutout c.II which is symmetric under reflections. This is a manifestation of the symmetry of the bilayer's intrinsic structure. If, however, the cutout boundaries do not respect the bi-layer's symmetry, e.g. b.III and b.IV, strips with a well defined handedness result, as seen in c.III, and c.IV. The handedness observed depends solely on the orientation of the strip's long axis; strips aligned with one diagonal generate right handed helicoids, whereas strips oriented in the perpendicular direction generate left handed helicoids. Slicing a narrow piece from a left handed strip such that its aspect ratio is inverted yields a narrower strip of opposite handedness as seen in c.V which was cut from c.VI.
The square cutout c.II holds the capacity to generate both right and left handed strips. We thus consider it as possessing both right and left handedness in equal amounts rather than having no handedness. It is right handed along the x direction, and left handed along the y direction. This directional dependence of the handedness is also observed in the relative positioning of cut-outs c.II, c.III and c.IV where the symmetric cutout c.II can be seamlessly continued in to manifestly Right or Left handed helical structures. Such an oriented dependent handedness cannot be captured by any pseudo-scalar measure and calls for quantification by a pseudo-tensor.

and left along the $\pm y$ directions, in agreement with the handedness of the elongated strips. In this way handedness emerges from a combination of the intrinsic structure of the bilayer and a choice of direction.

Neither (pseudo-)scalars nor (pseudo-)vectors are capable of capturing the orientational behavior described above. The simplest object that captures such an orientational variation is a (rank 2) pseudo-tensor such as the one shown in

Eq. 14:

$$\mathcal{X} = c \begin{pmatrix} 1 & 0 & 0 \\ 0 & -1 & 0 \\ 0 & 0 & 0 \end{pmatrix}. \tag{14}$$

This pseudotensor is symmetric under reflection, associates the x direction with a right (+) handed rotation about the x axis as observed in the χ_{xx} component, and associates the y direction with a left handed rotation (-) about the y axis as observed by the χ_{yy} component.

3.4 Tensorial handedness measures

We now seek to identify an orientation dependent handedness property, that in particular will be non-vanishing even for mirror symmetric cases. This requires us to broaden the notion of chirality. In order to determine the handedness of the each of the helicoidal strips in Figure 6 we followed the surface's face with the right hand. If advancing along the helicoid's length required the hand to roll outward, the helicoid was said to be right-handed. This related the rotation of the surface of the ribbon to its main axis direction. Optical activity, screw handedness as well as the chemists' R/S handedness descriptors for organic compounds all share this interpretation as relating directions to rotations. As directions are naturally vectors and rotations in $\mathbb{R}^3$ can be represented as pseudovectors relating the one to the other requires a pseudotensor. Constructing this pseudotensor requires us to identify the directions and the rotations the measure should relate.

In the case of embedded surfaces we consider a handedness measure that arises from a local handedness density χ^e. This handedness density pseudotensor is defined such that for every two unit vectors $\hat{\mathbf{n}}$ and $\hat{\mathbf{m}}$ we take the contraction $\hat{\mathbf{m}}\chi^e\hat{\mathbf{n}}$ to quantify the rotation of the surface's normal about the vector $\hat{\mathbf{m}}$ when it is displaced along the surface in the direction projected from $\hat{\mathbf{n}}$. It will be positive if the rotation about $\hat{\mathbf{m}}$ is right handed and negative when the associated rotation is left handed.

To formulate the above idea we start by considering a surface $\mathbf{r}$ parameterized by the coordinates x^α, where $\alpha = 1, 2$. These coordinates induce the metric $a_{\alpha\beta} = \partial_\alpha \mathbf{r} \cdot \partial_\beta \mathbf{r}$, and the second fundamental form $b_{\alpha\beta} = \partial_\alpha \partial_\beta \mathbf{r} \cdot \hat{\mathbf{N}}$, where $\hat{\mathbf{N}}$ is the surface's normal. Given a direction in space $\hat{\mathbf{n}}$ with cartesian component n_i we project it to the surface's tangent space by

$$\hat{\mathbf{n}}_\parallel = (\partial_\beta \mathbf{r} \cdot \hat{\mathbf{n}}) a^{\alpha\beta} \partial_\alpha \mathbf{r}.$$

Differentiating a function f defined on the surface along the projection of $\hat{\mathbf{n}}$ reduces to

$$(\hat{\mathbf{n}}_\parallel \cdot \nabla) f = (\partial_\beta \mathbf{r} \cdot \hat{\mathbf{n}}) a^{\alpha\beta} \partial_\alpha f.$$

For an oriented derivative of a vector field $(\hat{\mathbf{n}}\nabla)\mathbf{V}$ we may isolate the component which is due to a pure rotation about a vector $\hat{\mathbf{m}}$ by the scalar product $\hat{\mathbf{m}} \cdot \big(\hat{\mathbf{V}} \times (\hat{\mathbf{n}}\nabla)\mathbf{V}\big)$. Whenever this product is positive the change in the field $\mathbf{V}$ along $\hat{\mathbf{n}}$

is associated with a right handed rotation about $\hat{\mathbf{m}}$. The rotation of the normal of a surface about a vector $\hat{\mathbf{m}}$ when displaced along the direction induced by the vector $\hat{\mathbf{n}}$ is then given by

$$\hat{\mathbf{m}} \cdot \left(\hat{\mathbf{N}} \times ((\partial_\beta \mathbf{r} \cdot \hat{\mathbf{n}}) a^{\alpha\beta} \partial_\alpha \hat{\mathbf{N}})\right) = \hat{\mathbf{m}} \chi^e \hat{\mathbf{n}}, \tag{15}$$

where the chirality density, χ^e, defined by equation (15) can be rewritten in component form as

$$\chi^e_{ij} = \partial_\alpha r_j a^{\alpha\beta} \epsilon_{ilk} N^l \partial_\beta N^k, \tag{16}$$

where r_j and N^k denote the cartesian components of $\mathbf{r}$ and $\hat{\mathbf{N}}$ and ϵ is the antisymmetric Levi-Civita tensor. We may eliminate the normal vector from the formulation with the aid of the components of the second fundamental form $b_{\alpha\beta}$ and the two dimensional Levi Civita tensor $\epsilon^{\delta\gamma}$:

$$\chi^e_{ij} = \partial_\alpha r_j \partial_\delta r_i a^{\alpha\beta} b_{\gamma\beta} \epsilon^{\delta\gamma} / \sqrt{|a|}. \tag{17}$$

It is easy to show that the handedness density above transforms as a pseudo-tensor and is independent of the surface's parametrization and of the sign of the normal vector.

This handedness density may be integrated to give a tensorial handedness measure of the surface as a whole: $\mathcal{X}^e_{ij} = \iint \chi^e_{ij}\, dA$.

We note that this measure is traceless. This can be proved directly

$$\chi^e_{ii} = a_{\alpha\delta} a^{\alpha\beta} b_{\gamma\beta} \epsilon^{\delta\gamma} / \sqrt{|a|} = b_{\gamma\delta} \epsilon^{\delta\gamma} / \sqrt{|a|} = 0,$$

where the right equality follows from contracting a symmetric and antisymmetric tensor. This is in fact a hallmark of the local mirror symmetry of two dimensional surfaces. Every handedness density of the form $\chi_{ij} = \partial_\alpha r_j \partial_\beta r_i \tilde{\chi}^{\alpha\beta}$, where $\tilde{\chi}^{\alpha\beta}$ is a function of the local surface properties defined only through the first and second fundamental forms, a and b, must have a vanishing trace.

We would like to contrast this traceless measure with another measure that is not traceless. We do so by considering the handedness of an embedded curves following the same guiding principles described above. In this case the contraction $\hat{\mathbf{m}} \chi \hat{\mathbf{n}}$ gives the rotation of the curve's normal vector, $\mathbf{N}$, about the direction $\hat{\mathbf{m}}$ when displaced along the curve in the direction and magnitude projected from $\hat{\mathbf{n}}$.

We define $\mathbf{t}, \mathbf{N}$ and $\mathbf{b}$ to be a curve's tangent vector, normal vector and Binormal vector respectively. These unit vectors satisfy the Serret-Frenet formulas:

$$\partial_s \begin{pmatrix} \mathbf{t} \\ \mathbf{N} \\ \mathbf{b} \end{pmatrix} = \begin{pmatrix} 0 & \kappa & 0 \\ -\kappa & 0 & \tau \\ 0 & -\tau & 0 \end{pmatrix} \begin{pmatrix} \mathbf{t} \\ \mathbf{N} \\ \mathbf{b} \end{pmatrix},$$

where s is the arc-length parametrization of the curve and κ and τ are the curves curvature and torsion. Differentiating along the curve in direction projected from $\hat{\mathbf{n}}$ gives a weighted arc-length derivative $\mathbf{t} \cdot \hat{\mathbf{n}}\, \partial_s$. The handedness density tensor may be simplified by the Serret-Frenet equations to read

$$\chi_{ij} = t_i \epsilon_{jlk} N^l \partial_s N^k = t_i t_j \tau + t_i b_j \kappa. \tag{18}$$

The trace of the handedness density gives the local torsion, $\chi_{ii} = \tau$. For locally planar curves where $\tau = 0$ this gives a traceless tensor, as expected from the local mirror symmetry of such curves. In the general case, however, the measure is not traceless. For example when considering a helix oriented along the z axis of pitch p,

$$\mathbf{r} = \left[R\cos\left(\frac{s}{\sqrt{R^2+p^2}}\right), R\sin\left(\frac{s}{\sqrt{R^2+p^2}}\right), \frac{p\,s}{\sqrt{R^2+p^2}} \right],$$

then for an integer number of windings, M, the integrated handedness tensor is uniaxial and oriented along the axis of the helix:

$$\mathcal{X} = \begin{pmatrix} 0 & 0 & 0 \\ 0 & 0 & 0 \\ 0 & 0 & \frac{2\pi M\, p}{\sqrt{R^2+p^2}} \end{pmatrix} = \begin{pmatrix} 0 & 0 & 0 \\ 0 & 0 & 0 \\ 0 & 0 & \frac{\Delta Z}{\sqrt{R^2+p^2}} \end{pmatrix},$$

where ΔZ is the height of the helix.

Last we want want to construct a measure for a 3D unit vector field $\mathbf{u}$ such as used to describe the director field of a nematic or cholesteric mesophase of a liquid crystal. In this case we take the contraction $\hat{\mathbf{m}}\chi^e\hat{\mathbf{n}}$ to measure the rotation of the unit vector field $\mathbf{u}$ about the vector $\hat{\mathbf{m}}$ when displaced along the direction $\hat{\mathbf{n}}$. In components this takes the form

$$n^i \chi_{ij} m^j = n^i \partial_i u^k \epsilon_{jkl} u^l m^j.$$

The trace of the handedness tensor defined above gives

$$\chi^{ii} = \partial_i u^k \epsilon_{ikl} u^l = (\boldsymbol{\nabla} \times \mathbf{u}) \cdot \mathbf{u},$$

which coincides with the expression for helicity, c.f. magnetic helicity ($\mathbf{A} \cdot \mathbf{B} = \mathbf{A} \cdot (\nabla \times \mathbf{A})$), and hydrodynamic helicity ($\mathbf{u} \cdot \boldsymbol{\omega} = \mathbf{u} \cdot (\nabla \times \mathbf{u})$). Note that as the handedness density is quadratic in the unit vector field $\mathbf{u}$ it remains unchanged under the transformation $\mathbf{u} \to -\mathbf{u}$ allowing us to interpret $\mathbf{u}$ as a director field. For example a simple cholesteric order in which the director field is given by

$$\mathbf{u} = (\cos(pz), \sin(pz), 0),$$

displays a uniaxial handedness density oriented along the z direction

$$\chi = \begin{pmatrix} 0 & 0 & 0 \\ 0 & 0 & 0 \\ 0 & 0 & -p \end{pmatrix}.$$

In general, when this handedness measure is applied to director fields it yields not only the degree of handedness (such as the cholesteric pitch above), but also associates the handed phenomena with a direction.

3.5 A concluding remark about handedness and frustration

It is important to understand that we do not claim the existence of a single measure for handedness; we expect a plethora of handedness measures each applicable in it own setting measuring a specific handedness manifestation at a given scale. Nonetheless, we expect all such measures to be orientation dependent.

For the case of embedded surfaces we showed that the leading order handedness tensors will be traceless. However, this is not the case for rod-like objects (considered as 1D curves). If a natural system self assembles handed rod-like particles into surfaces we expect this assembly process to generate frustration. The purely right handed rods will inevitably give rise to both right and left handedness in the assembled surface.